

# Numerical analysis of flow and cavitation characteristics in a pilot-control globe valve with different valve core displacements<sup>\*</sup>

Jin-yuan QIAN<sup>1</sup>, Bu-zhan LIU<sup>1</sup>, Zhi-jiang JIN<sup>†‡1</sup>, Jian-kai WANG<sup>2</sup>, Han ZHANG<sup>3</sup>, An-le LU<sup>3</sup>

(<sup>1</sup>Institute of Process Equipment, College of Chemical and Biological Engineering, Zhejiang University, Hangzhou 310027, China)

(<sup>2</sup>China Tianchen Engineering Corporation, Tianjin 300400, China)

(<sup>3</sup>Shanghai Nuclear Engineering Research and Design Institute, Shanghai 200233, China)

<sup>†</sup>E-mail: jzj@zju.edu.cn

Received Aug. 17, 2015; Revision accepted Sept. 29, 2015; Crosschecked Dec. 11, 2015

**Abstract:** The pilot-control globe valve (PCGV) is a novel globe valve with a piston-type valve core and a small pilot valve. It can utilize a pressure difference to control the state of the main valve by the pilot valve. In this paper, a mathematical model of PCGV is established and a computational fluid dynamics (CFD) method is used to numerically simulate its flow and cavitation characteristics. Analysis of the pressure difference between the upside and downside of the valve core and comparison with similar previous work increase the reliability of the simulation. Then an analysis of flow and cavitation characteristics is carried out with three comparisons: a comparison between opened and closed states, a comparison between different inlet velocities, and a comparison between different valve core displacements. The results demonstrate that the vapor volume fraction reaches its peak point at the valve seat near the outlet tube, and that a higher inlet velocity or smaller valve core displacement can cause greater cavitation damage. This study can help further design work for optimization and engineering applications of PCGV.

**Key words:** Computational fluid dynamics (CFD), Pilot-control globe valve (PCGV), Valve core displacement, Cavitation  
<http://dx.doi.org/10.1631/jzus.A1500228>

**CLC number:** TH161.12

## 1 Introduction


As society advances, the globe valve is widely used in process industries for fluid control. However, its energy consumption is usually very large. To deal with that problem, we propose a novel globe valve, the pilot-control globe valve (PCGV), which can use a pressure difference to control the state of the main valve by means of a pilot valve. Instead of driving the

big valve core in the main valve directly, we use a pilot valve to realize the movement of the valve core; this can save a large amount of energy. In earlier work, we introduced the working principles of the PCGV, and analyzed by a numerical method the relationship between the valve core movement and different opening pressures, focusing on the dynamic flow characteristics (Qian *et al.*, 2014).

In the development of the valve, many researchers have done much useful work on analysis of the flow characteristics. Yang and Pan (2015) presented the recent developments and new techniques of valves in China. Many focused on specific valves with different structures or functions. Fu *et al.* (2007) analyzed the characteristics of flow through a throttling valve with different pressures. Palau-Salvador *et al.* (2008) carried out a 3D modeling of a control valve, and its geometrical influence on hydraulic

<sup>\*</sup> Corresponding author

<sup>\*</sup> Project supported by the National Natural Science Foundation of China (No. 51175454), the Key Scientific and Technological Innovation Team of Zhejiang Province, China (No. 2011R50005), and the Special Major Science and Technology Project of Zhejiang Province, China (Nos. 2012C11018-1 and 2012C11002)

 ORCID: Jin-yuan QIAN, <http://orcid.org/0000-0002-5438-0833>; Zhi-jiang JIN, <http://orcid.org/0000-0002-8063-709X>

© Zhejiang University and Springer-Verlag Berlin Heidelberg 2016

performance was observed. Chattopadhyay *et al.* (2012) investigated the flow through a spool type pressure regulating valve to analyze the flow structure inside it. Håkansson *et al.* (2012) developed an experimental technique to validate the  $k-\varepsilon$  Renault average Navier-Stokes model of a high-pressure homogenizer valve. Meanwhile, Dossena *et al.* (2013) paid attention to the performance of safety valves operating with different gases using both numerical and experimental methods. Jin *et al.* (2013) investigated a high parameter pressure-reducing valve by numerical simulation and carried out a structure optimization. Song *et al.* (2014) made a CFD analysis of a direct-operated safety relief valve on a pressure vessel. Saha *et al.* (2014) made a dynamic simulation of a pressure regulating and shut-off valve with different inlet pressures and positions of the spool. Mao *et al.* (2015) also made a dynamic numerical investigation of a valve seat subjected to the impact of the valve disc at low velocities. Furthermore, Simic and Herakovic (2015) presented the optimization of the spool and housing geometry in a small hydraulic seat valve, aiming to reduce axial flow forces to a minimum.

At the same time, cavitation characteristics were also investigated by many researchers in different types of valves because of the importance of cavitation damage to the valve body. Gao *et al.* (2002) made a numerical investigation of the cavitation flow behind the cone of a poppet valve in a water hydraulic system. An *et al.* (2008) made a numerical analysis of an anti-cavitation control valve used in a LNG marine system with different orifice diameters, and the newly designed valve in their work showed an improved flow pattern with reduced cavitation. Jazi and Rahimzadeh (2009) also studied the cavitation in a globe valve using waveform analysis. Meanwhile, Bernad and Susan-Resiga (2012) set up a numerical model of hydraulic poppet valves and investigated the cavitation flow inside the cavity. Margot *et al.* (2012) also presented validation and parametric studies of a numerical modelling of cavitation. Chern *et al.* (2013) carried out a numerical study on cavitation occurrence in a globe valve. In their work, the percentage of vapors in each computational cell was calculated by using a proposed cavitation model. Aung *et al.* (2014) researched a flapper-nozzle pilot valve numerically, and they also analyzed the cavitation phenomenon in an electrohydraulic servo-valve with an innovative

flapper shape (Aung and Li, 2014). Gholami *et al.* (2014) observed the cavitation phenomenon in a vaned ring-type needle valve by a numerical method. Amirante *et al.* (2014) analyzed the cavitation in a hydraulic proportional directional valve by experimental and numerical methods. Valdés *et al.* (2014) validated numerically and experimentally the cavitating flow through a ball check valve. Adamkowski and Lewandowski (2015) calculated the results of the water hammer course accompanied by column separation and observed the cavitation characteristics of shut-off valves in numerical modeling of transients in pipelines. Yaghoubi *et al.* (2015) focused on the different numbers of anti-cavitation trims in a globe valve to check its influence on the cavitation phenomenon.

In this paper, to further research the flow and cavitation characteristics of PCGV, we simulate the pressure difference between the upside and downside of the valve core, and we first compare it with similar previous work to increase the reliability of the simulation. Then analysis of flow and cavitation characteristics is carried out by three comparisons: a comparison between opened and closed states, a comparison between different inlet velocities, and a comparison between different valve core displacements. This work can support design work for further optimization and engineering applications of PCGV.

## 2 Numerical model

### 2.1 Mathematical model

Since the actual movements of the fluid inside PCGV are very complex, we adopt the RNG  $k-\varepsilon$  turbulence model for its advantage in dealing with high strain rate and streamline curvature. In the cavitation case, phase change occurs between the liquid phase and vapor phase. Thus, the mixture continuity and momentum equations are shown as

$$\frac{\partial}{\partial t} \rho_m + \nabla(\rho_m \mathbf{v}) = 0, \quad (1)$$

$$\begin{aligned} \frac{\partial}{\partial t} (\rho_m \mathbf{v}) = & -\nabla p + \nabla \cdot [(\mu_m + \mu_t) \nabla \mathbf{v}] \\ & + \frac{1}{3} \nabla[(\mu_m + \mu_t) \nabla \cdot \mathbf{v}] - \nabla(\rho_m \mathbf{v} \mathbf{v}), \end{aligned} \quad (2)$$

$$\rho_m = \alpha \rho_v + (1 - \alpha) \rho_l, \quad (3)$$

$$\mu_m = \alpha \mu_v + (1 - \alpha) \mu_l, \quad (4)$$

where  $\rho_m$ ,  $\rho_v$ , and  $\rho_l$  represent the mixture, vapor, and liquid densities, respectively;  $\mathbf{v}$  is the velocity vector;  $\mu_m$ ,  $\mu_v$  and  $\mu_l$  represent the mixture, vapor, and liquid kinetic viscosities, respectively, and  $\mu_t$  is the turbulent viscosity;  $p$  is the pressure;  $\alpha$  is the vapor volume fraction.

The cavitation model we used is based on the Rayleigh-Plesset equation. Although the compressibility of liquid is very important when bubbles break, here we assume  $\rho_l$  as a constant and so are  $\mu_l$ ,  $\rho_v$ , and  $\mu_v$ . Meanwhile, we assume the bubbles remain spherical and there is no thermal conductivity with tubes linked with PCGV. Thus, the liquid vapor mass transfer is governed by

$$\frac{\partial}{\partial t}(\alpha \rho_v) + \nabla(\alpha \rho_v \mathbf{v}) = R_c - R_b, \quad (5)$$

$$R_c = \frac{3\alpha \rho_v (1 - \alpha) \rho_l}{\rho R_b} \sqrt{\frac{2(p_v - p)}{3\rho_l}}, \quad p_v \geq p, \quad (6)$$

$$R_c = \frac{3\alpha \rho_v (1 - \alpha) \rho_l}{\rho R_b} \sqrt{\frac{2(p - p_v)}{3\rho_l}}, \quad p_v \leq p, \quad (7)$$

where  $R_c$  and  $R_b$  are the rates of growth and breaking of vapor bubbles, respectively;  $R_b$  is the bubble radius;  $p_v$  is the saturation pressure of water.

## 2.2 Geometrical model

In earlier work (Qian *et al.*, 2014), we introduced the detailed working principles of the PCGV. Therefore, we only describe its key parts briefly. As is shown in Fig. 1, compared with the traditional globe valve, PCGV has a pilot valve, which can be a manual ball valve, an electric ball valve, or a magnetic valve, etc. Here, the valve core is a piston type with a spring. With the control of the pilot valve, the piston type valve core can move up and down to control the opening and closing states of the main valve by using the pressure difference before and after the main valve. It has a very obvious advantage of energy conservation since the PCGV does not need to drive the large valve core directly, but utilizes the small pilot valve instead.

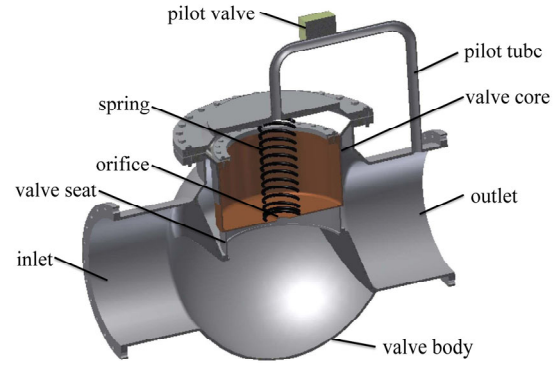


Fig. 1 Pilot-control globe valve and its key parts

To enable numerical analysis, some simplification is carried out. Firstly, we assume that PCGV is an ideal valve, which means that its cutting edge is a right angle exactly with sharp edges, and the valve core matches the valve seat precisely. Then, to save computation time, we use a 3D axisymmetric geometric model by considering the symmetry structure. Also, we do not consider the impact of the spring inside because it has little effect on the internal flow field.

In addition, to reduce the effects of the connection point between the pilot tube and the main valve, we assume that fluid does not re-enter the main valve, but flows directly out of the pilot valve, and we also take no account of the effects of gravity and heat transfer.

## 2.3 Mesh and boundary condition

Fig. 2 shows the mesh of DN100 PCGV with valve core displacement of 25 mm. The diameter of the piston type valve core is 100 mm and we set the diameter of the orifice as 4 mm according to our experience. Another four models of DN100 PCGV with valve core displacements of 5 mm, 10 mm, 15 mm, and 20 mm are also developed. To enhance the accuracy of simulation, we leave an area of one diameter ( $D$ ) before the valve inlet and two diameters after the valve outlet. These parts are meshed with structured grids, while, because of its complex structure, the main part is divided using a non-structured mesh partition.

The grid independence check is carried out under the opened condition. We take the pressure difference as the judgment parameter with different

interval sizes from 2 mm to 10 mm. As shown in Table 1, when the interval size ranges between 2 mm and 6 mm, the relative errors of the simulation keep within 2%, so we choose 6 mm as the interval size. In addition, we use an adaptive grids function to optimize the mesh quality according to the numerical results and geometry. The pressure differences at the orifice, valve core, and valve seat differ a lot, which leads to cavitation. Therefore, we do a further simulation with the internal flow field pressure gradient as the adaptive function. After every specified number of iterations, the adaption is operated.

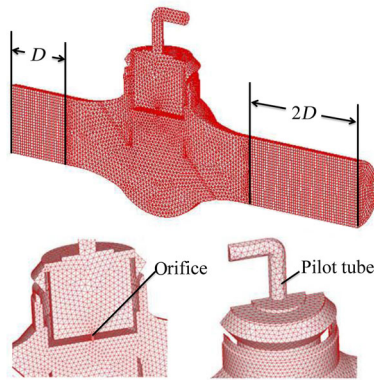


**Fig. 2** Mesh of PCGV with valve core displacement of 25 mm

**Table 1** Pressure difference under different interval size

Interval size (mm)	Pressure difference (kPa)
10	189.2
8	169.1
6	163.4
4	163.1
2	162.9

For the boundary conditions, the inlet condition of PCGV is the velocity inlet condition, and the outlet condition is the pressure outlet condition. For the pilot tube outlet, it is set to the pressure outlet condition while open and as the wall while closed. The wall function method is adopted in the near wall region by using the finite volume method and first-order upwind scheme. Coupling pressure and velocity is based on SIMPLE. In addition, incompressible liquid water is chosen as the liquid phase while water vapor is chosen as the vapor phase. In the simulation,  $\rho_l$  and  $\rho_v$

are set as  $998.2 \text{ kg/m}^3$  and  $0.55 \text{ kg/m}^3$ , and  $\mu_l$  and  $\mu_v$  are set as  $1.003 \times 10^{-3} \text{ N}\cdot\text{s/m}^2$  and  $1.34 \times 10^{-5} \text{ N}\cdot\text{s/m}^2$ , respectively.

### 3 Results and discussion

To analyze the flow and cavitation characteristics of PCGV under different conditions for the whole process, we developed all 10 models of opened and closed states with valve core displacements of 5 mm, 10 mm, 15 mm, 20 mm, and 25 mm. In these models, the flow field, pressure field, and vapor distributions are studied. We make a comparison with some similar studies focusing on the pressure difference of valves, for the purpose of checking the accuracy of the simulation. Then, flow and cavitation characteristics of opened and closed states are studied. Furthermore, we study the influence of inlet velocity on the flow and cavitation characteristics. Finally, we analyze the cavitation characteristics with different valve core displacements.

#### 3.1 Comparison with similar simulations

Pressure difference is one of the most important factors in the opening and closing processes of valves. To check the accuracy of the simulation work, the pressure difference of PCGV under different conditions is studied. We take the inlet velocity 3 m/s as an example. Focusing on the pressure on the upper and lower surfaces of the valve core, we can get an average upper surface pressure and an average lower surface pressure. The difference between them is the total pressure difference. It is worth mentioning that their directions are opposite. During the opened state, the pressure difference is upward while during the closed state, the pressure difference is downward.

The pressure difference under different valve core displacements is shown in Table 2. The largest opened pressure difference and closed pressure difference are both located at 5 mm of valve core displacement and at that time the valve core has the largest acceleration.

Meanwhile, both opened and closed pressure differences decrease with the increase of the valve core displacement, and the variation range also decreases when the valve core displacement changes from 5 mm to 25 mm. Fig. 3 shows the fluid force

during the change of the valve core displacement, presenting the results more directly.

**Table 2 Pressure difference under different valve core displacement**

Valve core displacement (mm)	Opened pressure difference (kPa)	Closed pressure difference (kPa)
5	163.4	30.4
10	69.9	10.1
15	32.1	7.5
20	24.5	6.0
25	18.3	4.2

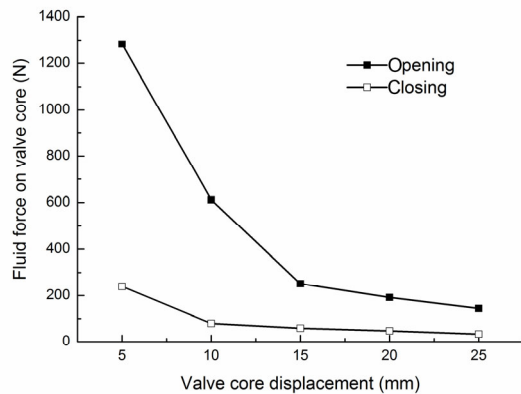


**Fig. 3 Fluid force under different valve core displacements when inlet velocity is 3 m/s**

Here, we compare the simulation result with a similar valve (Fu *et al.*, 2008). Those authors did numerical and experimental research on an electro-hydraulic proportional cartridge valve. They presented their simulation study of valve core displacement under the effects of orifice, spool section, stiffness of feedback spring, etc. Comparing these figures with our previous study (Qian *et al.*, 2014) we find similar movement principles although PCGV has different structures and different influence parameters from the electro-hydraulic proportional cartridge valve. In addition, they mentioned that, for a similar size of valve, the pressure difference is 0.5 MPa when the flow rate is 10.8 m/s. In our simulation, the inlet velocity is 3 m/s. We note the square relationship between pressure difference and the inlet velocity. From Table 2, it can be seen that our simulation results of pressure difference have the same order of magnitude under the valve core displacement from 5 mm to 25 mm. To further improve reliability, we

also compare PCGV with another globe valve (Chern *et al.*, 2013). In the grid independency test of various meshes, Chern *et al.* (2013) also chose the pressure difference as the judgment parameter, ranging from 17.3 kPa to 21.3 kPa under similar conditions. Moreover, in a control valve (Palau-Salvador *et al.*, 2008), with similar inlet velocities, they found that the pressure different inside changes from 0.2 MPa to 1.4 MPa. Though these published experimental or numerical data cannot validate our model directly, this comparison suggests reliability of our results and the correctness of the simulation.

### 3.2 Comparison between opened and closed states

The conditions of the model we analyze are as follows: the valve core displacement is 25 mm, the inlet velocity is 3 m/s, and the outlet pressure is 0 MPa. As shown in Fig. 4, Figs. 4a and 4b are the velocity contours at symmetrical and longitudinal sections at opened state, while Figs. 4c and 4d are the velocity contours at symmetrical and longitudinal sections at closed state. Meanwhile, Figs. 5a–5d also shows the cavitation characteristics at symmetrical and longitudinal sections at opened and closed states.

Though the flow inside PCGV is very complex, the velocity and the vapor volume fraction remain relatively stable at the inlet and outlet. As shown in Fig. 4, in the inlet part, the velocity keeps approximately to 3 m/s in both opened and closed states. Meanwhile in the outlet part, after a full development with a length of two diameters, the velocity is approximately 3 m/s in both opened and closed states. For the vapor volume fraction, at both states, the inlet and outlet parts have a relatively stable vapor volume fraction, about 0.85% and 1.35%, respectively. At the same time, along with the direction of fluid flow, the flow and cavitation characteristics reach agreement at longitudinal sections.

In the opened state, the fluid divides into two parts under the valve core. One part flows through the orifice with an increasing velocity, up to 4.5 m/s, into the cavity of the valve core, and then flows through the pilot tube. Because of the increasing velocity of this part, there is a pressure difference produced which pushes the valve core upward.

As is shown in Figs. 5a and 5b, in the cavity of the valve, the cavitation phenomenon remains steady with a vapor volume fraction of 1.40%. The other part



of the fluid flows directly to the outlet, and at the point of the valve seat before the outlet tube, the velocity and the vapor volume fraction reaches the peak

point, at about 6.50 m/s and 1.55%, respectively. Then, the velocity decreases and the vapor volume fraction are slightly reduced but stable.

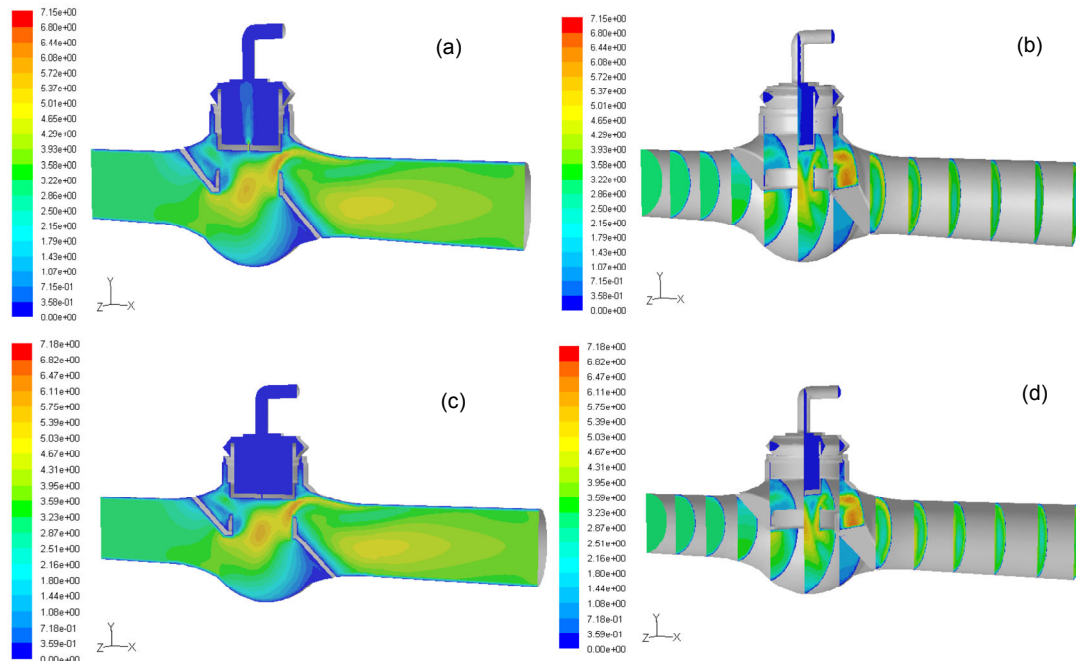


**Fig. 4** Velocity contours under opened and closed states with valve core displacement of 25 mm, inlet velocity of 3 m/s (a) Symmetrical, opened; (b) Longitudinal, opened; (c) Symmetrical, closed; (d) Longitudinal, closed (unit: m/s)

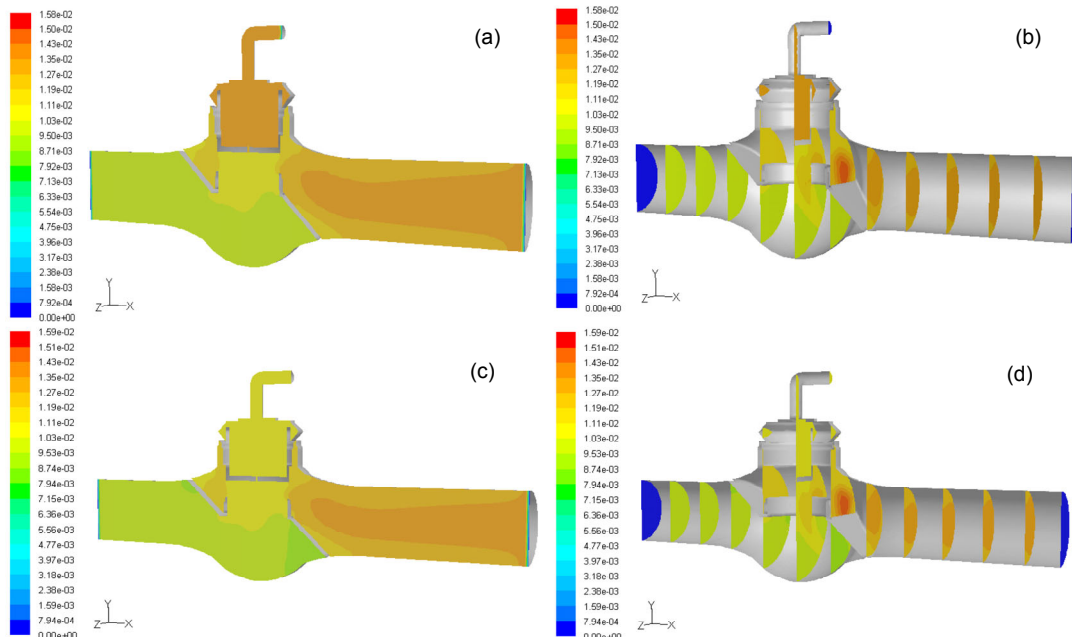


**Fig. 5** Vapor volume fraction contours under opened and closed states with valve core displacement of 25 mm, inlet velocity of 3 m/s

(a) Symmetrical, opened; (b) Longitudinal, opened; (c) Symmetrical, closed; (d) Longitudinal, closed (unit: %)

In the closed state, except at the orifice, the flow and cavitation characteristics at the other part are the same as in the opened state. However, due to the closure of the pilot valve, the outlet of the pilot tube is set as wall, which means the fluid there has no velocity, and there is no fluid flowing through the pilot tube. Therefore, the vapor volume fraction is a little lower, about 1.10% compared with about 1.35% in the opened state.

From these comparisons, we can see that, in both opened and closed states, at the point of the valve seat before the outlet tube, the velocity and the vapor volume fraction reach a peak, which means that the valve seat before the outlet tube is the part most vulnerable to cavitation. Meanwhile, although there is a throttle at the orifice part, it seems that there is no need to take the orifice into consideration since the

vapor volume fraction there is much lower than that at the valve seat before the outlet tube.

### 3.3 Comparison between different inlet velocities

For this part, the conditions of the model we analyze are as follows: the valve core displacement is 25 mm, the inlet velocity is 2 m/s or 4 m/s, and the outlet pressure is 0 MPa in the closed state. As is shown in Fig. 6, Figs. 6a and 6b are the pressure contours at symmetrical sections with 2 m/s and 4 m/s, while Figs. 6c and 6d are the velocity contours, and Figs. 6e and 6f are the vapor volume fraction contours of 2 m/s and 4 m/s, respectively.

Comparing the pressure contours and the velocity contours, we find that they have similar contours but with different magnitudes. As we can see, for the inlet and outlet, it also remains stable with their initial

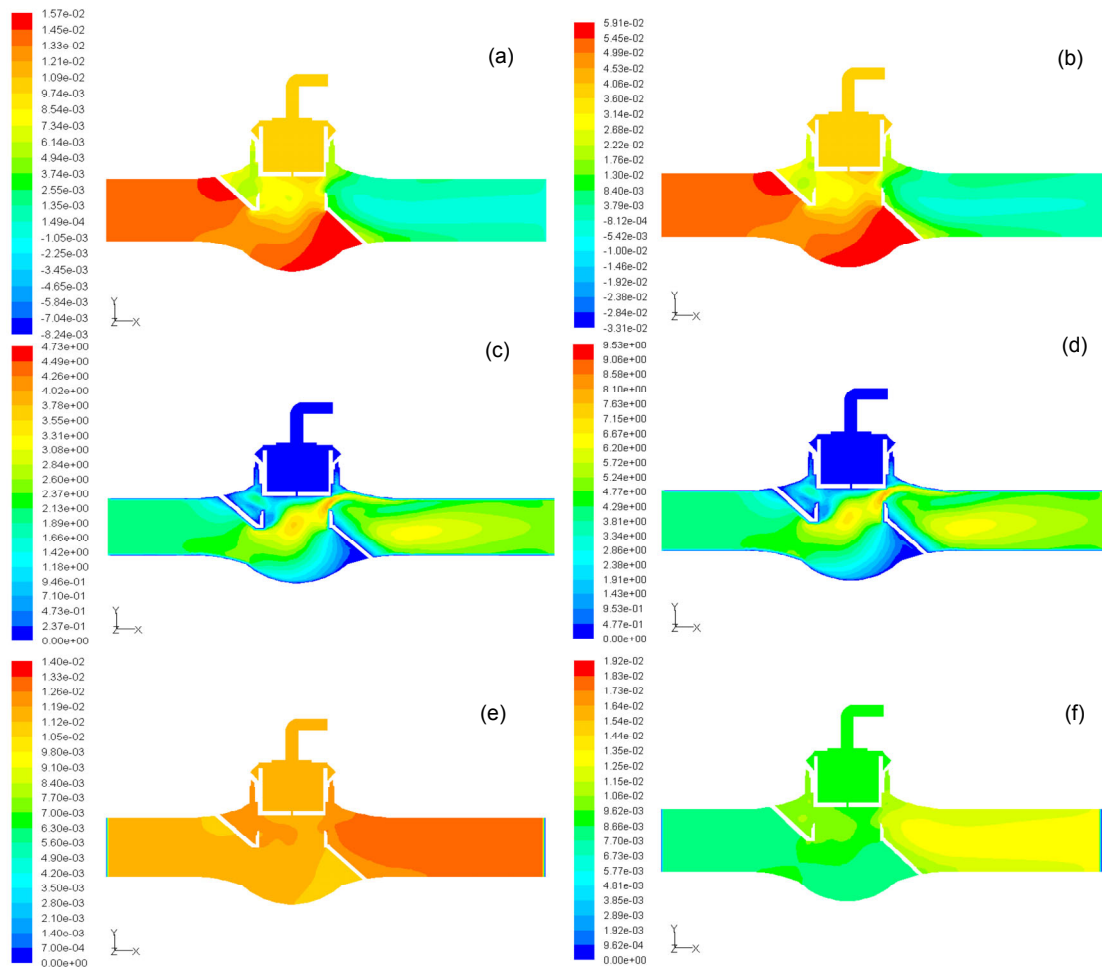


**Fig. 6** Pressure, velocity, and vapor volume fraction contours under closed states with inlet velocities of 2 m/s and 4 m/s (a) Pressure, 2 m/s; (b) Pressure, 4 m/s; (c) Velocity, 2 m/s; (d) Velocity, 4 m/s; (e) Vapor volume fraction, 2 m/s; (f) Vapor volume fraction, 4 m/s. The units of pressure, velocity, and vapor volume fraction are Pa, m/s, and %, respectively

velocities, just as is mentioned in section 3.2.1. With the higher inlet velocity at 4 m/s, the total velocity inside is also higher with a peak velocity of about 9.50 m/s. When the inlet velocity is 2 m/s, the peak velocity is only about 4.70 m/s. There is a similar ratio between the pressure differences between the upside and downside of the valve core. Thus, with the higher inlet velocity, PCGV opens more quickly since the pressure difference is much higher. The movement of the valve core is thus assisted.

Meanwhile, due to the increased pressure difference, the ranges of distribution of vapor volume fraction increase, from 1.12%–1.40% at 2 m/s to 0.70%–1.90% at 4 m/s, which means a greater likelihood of cavitation damage to the valve body with the higher velocities. Under most conditions, a higher

inlet velocity causes higher cavitation damage. However, when there is a higher inlet velocity, the pressure at the inlet is also higher, which can inhibit the generation of cavitation. We repeated these simulations for the opened state with similar results.

### 3.4 Comparison between different valve core displacements

We analyze the influence on the flow and cavitation characteristics with different valve core displacements, by setting the conditions of the model as follows: the valve core displacement is 10 mm or 20 mm, the inlet velocity is 3 m/s, and the outlet pressure is 0 MPa in the opened state. As shown in Fig. 7, Figs. 7a and 7b are the pressure contours at symmetrical sections of 10 mm and 20 mm, while

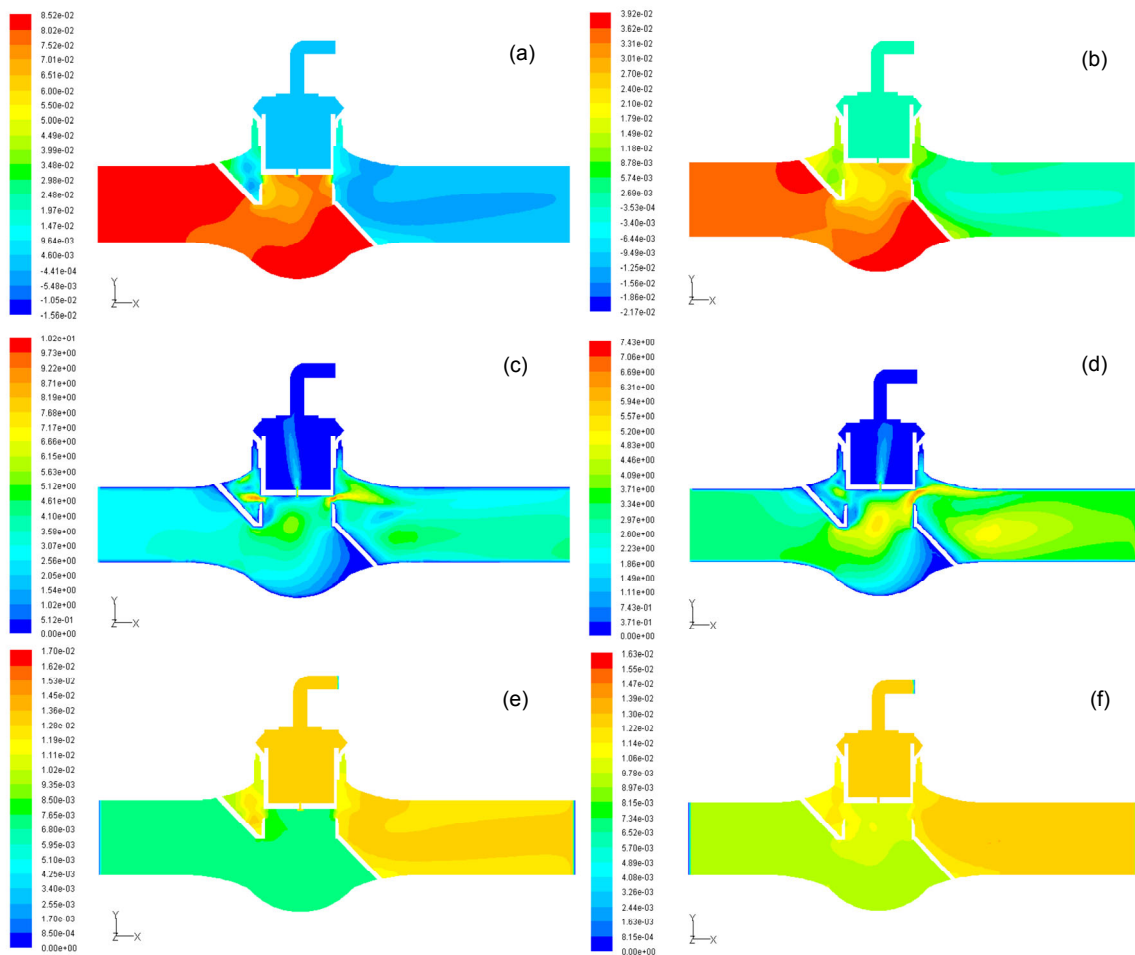


**Fig. 7** Pressure, velocity, and vapor volume fraction contours under opened states with valve core displacements of 10 mm and 20 mm

(a) Pressure, 10 mm; (b) Pressure, 20 mm; (c) Velocity, 10 mm; (d) Velocity, 20 mm; (e) Vapor volume fraction, 10 mm; (f) Vapor volume fraction, 20 mm. The units of pressure, velocity, and vapor volume fraction are Pa, m/s, and %, respectively



Figs. 7c and 7d are the velocity contours, and Figs. 7e and 7f are the vapor volume fraction contours for 10 mm and 20 mm, respectively.

From Fig. 7, we can see different valve core displacements under different distributions of flow and cavitation. When the displacement is smaller at 10 mm, the pressure difference is larger. This can also explain the working principle of PCGV during the opened state. If the balance is not reached, the valve core will keep moving upward. At that time, although the peak velocity at the valve seat is relatively high, about 10 m/s, the rate of flow is not as large as the velocity, so that the influence on the outlet tube is not as obvious as that at the higher displacement.

However, when the displacement is 20 mm, although the pressure difference is small and the peak velocity at the valve seat is about 7.40 m/s, the rate of flow is very large so that the influence on the outlet tube is very obvious. It is worth mentioning that at both 10 mm and 20 mm of valve core displacement, there is always a part with no velocity; that is located at the bottom of the main valve in the outlet direction. This part may suffer corrosion easily and is not easy to clean, and we need to further optimize it.

Meanwhile, comparing Fig. 7e with Fig. 7f, we can see that when there is a smaller displacement, the vapor volume fraction is higher, especially in the part before the valve core, but the difference is not great. In addition, we deal with the simulation in the closed state, and the simulation results agree with those of the open state, that is to say that smaller valve core displacements are associated with more cavitation damage. From this comparison work, we can see that, during design work on the limited structure, we should try to choose a suitable spring to make the operating position as high as possible.

#### 4 Conclusions

By analysis of the pressure difference between the upside and downside of the valve core, the possibility of the movement of the valve core in PCGV is presented. Meanwhile, the comparison with some similar studies increases the reliability and the accuracy of the simulation.

In the open state, fluid from inlet divides into two parts, one through the orifice into the cavity of the

valve core and the other through the valve seat to the outlet. In the closed state, since there are no fluid flows through the pilot tube, the vapor volume fraction is a little lower during the closed time; except for that the flow and cavitation in other parts look the same as in the open state. At both opened and closed states, at the point of the valve seat before the outlet tube, the velocity and the vapor volume fraction reach their peak, which means that the valve seat before the outlet tube part is the part most liable to cavitation. Thus, in manufacture, material at this part should be strengthened by hardening.

The contours of velocity, pressure, and the vapor volume fraction seem similar when there are different inlet velocities, but with a higher inlet velocity the total velocity inside are also higher. Thus, with a higher inlet velocity, PCGV can open more quickly since the pressure difference is much higher, and that is useful for the movement of the valve core. Meanwhile, with the increase in inlet velocity, the range of distribution of vapor volume fractions increases, but a greater cavitation does not follow because when there is a higher inlet velocity, the pressure in the inlet part is also higher, and that higher pressure can inhibit the generation of cavitation.

Flow and cavitation with different valve core displacements seem to differ. When the displacement is small, the pressure difference is large, which again explains the working principle of the PCGV when opened. Though the velocity at the valve seat is relatively high when there is a small valve core displacement, the influence on the outlet tube is not obvious due to the relatively small rate of flow. However, the pressure gradient is larger giving a higher vapor volume fraction and higher cavitation damage under smaller valve core displacement. Thus, during the design work of limited structure, we should try to choose a suitable spring to make the operating position as high as possible.

Besides, in PCGV, there always exists a part with no velocity at the bottom of the main valve in the outlet direction, and this part may suffer corrosion easily, so that further optimization is needed. In addition, although there exist a throttle at the orifice part, it seems that there is no need to take the orifice into consideration since the vapor volume fraction is much lower than that in the valve seat before the outlet tube part.

In this study, we take no consideration of the size of the orifice but from experience, further research on its size might be useful. This flow and cavitation analysis work on PCGV can guide the optimization and production process to further help its engineering application.

## References

- Adamkowski, A., Lewandowski, M., 2015. Cavitation characteristics of shutoff valves in numerical modeling of transients in pipelines with column separation. *Journal of Hydraulic Engineering*, **141**(2):04014077.  
[http://dx.doi.org/10.1061/\(ASCE\)HY.1943-7900.0000971](http://dx.doi.org/10.1061/(ASCE)HY.1943-7900.0000971)
- Amirante, R., Distaso, E., Tamburrano, P., 2014. Experimental and numerical analysis of cavitation in hydraulic proportional directional valves. *Energy Conversion and Management*, **87**:208-219.  
<http://dx.doi.org/10.1016/j.enconman.2014.07.031>
- An, Y.J., Kim, B.J., Shin, B.R., 2008. Numerical analysis of 3-D flow through LNG marine control valves for their advanced design. *Journal of Mechanical Science and Technology*, **22**(10):1998-2005.  
<http://dx.doi.org/10.1007/s12206-008-0745-6>
- Aung, N.Z., Li, S., 2014. A numerical study of cavitation phenomenon in a flapper-nozzle pilot stage of an electrohydraulic servo-valve with an innovative flapper shape. *Energy Conversion and Management*, **77**:31-39.  
<http://dx.doi.org/10.1016/j.enconman.2013.09.009>
- Aung, N.Z., Yang, Q., Chen, M., et al., 2014. CFD analysis of flow forces and energy loss characteristics in a flapper-nozzle pilot valve with different null clearances. *Energy Conversion and Management*, **83**:284-295.  
<http://dx.doi.org/10.1016/j.enconman.2014.03.076>
- Bernad, S.I., Susan-Resiga, R., 2012. Numerical model for cavitation flow in hydraulic poppet valves. *Modelling and Simulation in Engineering*, **2012**:742162.  
<http://dx.doi.org/10.1155/2012/742162>
- Chattopadhyay, H., Kundu, A., Saha, B.K., et al., 2012. Analysis of flow structure inside a spool type pressure regulating valve. *Energy Conversion and Management*, **53**(1):196-204.  
<http://dx.doi.org/10.1016/j.enconman.2011.08.021>
- Chern, M., Hsu, P., Cheng, Y., et al., 2013. Numerical study on cavitation occurrence in globe valve. *Journal of Energy Engineering*, **139**(1):25-34.  
[http://dx.doi.org/10.1061/\(ASCE\)EY.1943-7897.0000084](http://dx.doi.org/10.1061/(ASCE)EY.1943-7897.0000084)
- Dossena, V., Marinoni, F., Bassi, F., et al., 2013. Numerical and experimental investigation on the performance of safety valves operating with different gases. *International Journal of Pressure Vessels and Piping*, **104**:21-29.  
<http://dx.doi.org/10.1016/j.ijpvp.2013.01.002>
- Fu, L., Wei, J., Qiu, M., 2008. Dynamic characteristics of large flow rating electro-hydraulic proportional cartridge valve. *Chinese Journal of Mechanical Engineering (English Edition)*, **21**(06):57-62.  
<http://dx.doi.org/10.3901/CJME.2008.06.057>
- Fu, X., Du, X., Zou, J., et al., 2007. Characteristics of flow through throttling valve undergoing a steep pressure gradient. *International Journal of Fluid Power*, **8**(1):29-37.  
<http://dx.doi.org/10.1080/14399776.2007.10781265>
- Gao, H., Fu, X., Yang, H.Y., et al., 2002. Numerical investigation of cavitating flow behind the cone of a poppet valve in water hydraulic system. *Journal of Zhejiang University-SCIENCE*, **3**(4):395-400.  
<http://dx.doi.org/10.1631/jzus.2002.0395>
- Gholami, H., Yaghoubi, H., Alizadeh, M., 2014. Numerical analysis of cavitation phenomenon in a vaned ring-type needle valve. *Journal of Energy Engineering*, **141**(4):04014053.  
[http://dx.doi.org/10.1061/\(ASCE\)EY.1943-7897.0000255](http://dx.doi.org/10.1061/(ASCE)EY.1943-7897.0000255)
- Håkansson, A., Fuchs, L., Innings, F., et al., 2012. Experimental validation of  $k-\epsilon$  RANS-CFD on a high-pressure homogenizer valve. *Chemical Engineering Science*, **71**:264-273.  
<http://dx.doi.org/10.1016/j.ces.2011.12.039>
- Jazi, A.M., Rahimzadeh, H., 2009. Waveform analysis of cavitation in a globe valve. *Ultrasonics*, **49**(6-7):577-582.  
<http://dx.doi.org/10.1016/j.ultras.2009.02.004>
- Jin, Z.J., Wei, L., Chen, L.L., et al., 2013. Numerical simulation and structure improvement of double throttling in a high parameter pressure reducing valve. *Journal of Zhejiang University-SCIENCE A (Applied Physics & Engineering)*, **14**(2):137-146.  
<http://dx.doi.org/10.1631/jzus.A1200146>
- Mao, J., Wang, W., Zhang, J., et al., 2015. Numerical investigation on the dynamic behaviors of turbine valve disc-seat impact at low velocity. *Journal of Mechanical Science and Technology*, **29**(2):507-515.  
<http://dx.doi.org/10.1007/s12206-015-0111-4>
- Margot, X., Hoyas, S., Gil, A., et al., 2012. Numerical modeling of cavitation: validation and parametric studies. *Engineering Applications of Computational Fluid Mechanics*, **6**(1):15-24.  
<http://dx.doi.org/10.1080/19942060.2012.11015399>
- Palau-Salvador, G., Gonzalez-Altozano, P., Arviza-Valverde, J., 2008. Three-dimensional modeling and geometrical influence on the hydraulic performance of a control valve. *Journal of Fluids Engineering*, **130**(1):011102.  
<http://dx.doi.org/10.1115/1.2813131>
- Qian, J.Y., Wei, L., Jin, Z.J., et al., 2014. CFD analysis on the dynamic flow characteristics of the pilot-control globe valve. *Energy Conversion and Management*, **87**:220-226.  
<http://dx.doi.org/10.1016/j.enconman.2014.07.018>
- Saha, B.K., Chattopadhyay, H., Mandal, P.B., et al., 2014. Dynamic simulation of a pressure regulating and shut-off valve. *Computers & Fluids*, **101**:233-240.  
<http://dx.doi.org/10.1016/j.compfluid.2014.06.011>
- Simic, M., Herakovic, N., 2015. Reduction of the flow forces in a small hydraulic seat valve as alternative approach to improve the valve characteristics. *Energy Conversion and Management*, **89**:708-718.  
<http://dx.doi.org/10.1016/j.enconman.2014.10.037>

- Song, X., Cui, L., Cao, M., *et al.*, 2014. A CFD analysis of the dynamics of a direct-operated safety relief valve mounted on a pressure vessel. *Energy Conversion and Management*, **81**:407-419.  
<http://dx.doi.org/10.1016/j.enconman.2014.02.021>
- Valdés, J.R., Rodríguez, J.M., Monge, R., *et al.*, 2014. Numerical simulation and experimental validation of the cavitating flow through a ball check valve. *Energy Conversion and Management*, **78**:776-786.  
<http://dx.doi.org/10.1016/j.enconman.2013.11.038>
- Yaghoubi, H., Adib, A.A., Madani, S., *et al.*, 2015. A numerical analysis of cavitation phenomenon in a globe valve with different numbers of anti-cavitation trims. *Journal of Zhejiang University-SCIENCE A (Applied Physics & Engineering)*, in press.  
<http://dx.doi.org/10.1631/jzus.A1400258>
- Yang, H.Y., Pan, M., 2015. Engineering research in fluid power: a review. *Journal of Zhejiang University-SCIENCE A (Applied Physics & Engineering)*, **16**(6): 427-442.  
<http://dx.doi.org/10.1631/jzus.A1500042>

## 中文概要

**题 目:** 先导式截止阀在不同阀芯位置下流动和汽蚀特性的数值分析

**目 的:** 先导式截止阀可通过一个先导阀, 利用流体在阀

门前后自身的压差控制主阀的启闭, 是一种新型节能型截止阀。本文探讨该阀在开启和关闭状态下、不同入口速度情况下和不同阀芯位置下的流动和汽蚀特性, 为后期结构优化提供设计建议。

**创新点:** 1. 分析先导式截止阀的阀芯上下表面压差的变化情况, 验证其可行性和模型准确性; 2. 建立数值模型, 对先导式截止阀在不同启闭状态和不同阀芯位移情况下进行流动和汽蚀分析。

**方 法:** 1. 通过数值模拟, 分析阀芯上下表面的压差, 并与现有文献进行比较, 验证模型的准确性(图 3); 2. 建立开启和关闭条件下的阀门模型, 比较两种状态下该阀的流动和汽蚀特性(图 4 和 5); 3. 建立不同入口速度条件下的阀门模型, 比较分析速度对该阀的汽蚀情况的影响(图 6); 4. 建立不同阀芯位置的阀门模型, 比较分析不同阀芯位置下的速度和压力情况, 进一步验证该阀的可行性, 并分析阀芯位置对阀门汽蚀的影响(图 7)。

**结 论:** 1. 在开启和关闭状态下, 流速和汽含率在阀座底部靠近出口处达到峰值; 2. 入口速度更高的情况下, 阀的开启速度更快, 但汽含率并不一定同步上升; 3. 当阀芯处于低位置时, 虽然对阀门出口处影响位置较小, 但其压力梯度较大、汽含率较高, 选取合适的弹簧刚度非常重要。

**关键词:** 计算流体动力学; 先导式截止阀; 阀芯位移; 汽蚀